Doping dependence of the in-plane penetration depth and fishtail in $Bi_2Sr_2Ca_{1-x}Y_xCu_2O_{8+\delta}$ single crystals

G. Villard, D. Pelloquin, and A. Maignan
Laboratoire CRISMAT, ISMRA et Université de Caen, Unité Mixte de Recherche (UMR 6508) associée au CNRS, 6 Bd du Maréchal Juin, 14050 Caen Cedex, France
(Received 7 April 1998)

We report on the London penetration depth $\lambda_{ab}(0)$, measurements, and second peak $\tilde{H}$ determination in $Bi_2Sr_2Ca_{1-x}Y_xCu_2O_{8+\delta}$ (Bi-2212) crystals with different doping levels. By combining cationic substitutions and oxygen pressure annealings, crystals with a doping state going from the underdoped to overdoped regime have been obtained. The corresponding $\lambda_{ab}(0)$ values, deduced from reversible magnetization measurements have allowed us to evidence a ''boomerang'' shape for the $T_c[1/\lambda_{ab}^2(0)]$ curve in the $0.8 \leqslant T_c/T_c^{\max} \leqslant 1$ region. Moreover, other $T_c[1/\lambda_{ab}^2(0)]$ values for superconducting crystals of Hg- and Tl-based cuprates are found to fit well with this boomerang path, demonstrating its universal nature. The overdoped side of the boomerang for the Bi-2212 crystals clearly shows that $1/\lambda_{ab}^2(0)$ decreases as the doping level is increased. Since by the same time the characteristic field of the fishtail $\tilde{H}$ monotonously increases, we have thus established that $\tilde{H}$ increases with $1/\lambda_{ab}^2(0)$ decreasing. Consequently, the linear relation $\tilde{H}=\Phi_0/\lambda_{ab}^2(0)$ predicted by the electromagnetic model cannot account alone for the present experimental results in the overdoped regime.
[S0163-1829(98)04546-9]

I. INTRODUCTION

In recent years, the large number of studies devoted to the superconducting cuprate $Bi_2Sr_2CaCu_2O_{8+\delta}$ (Bi-2212) have enlightened the peculiar behavior of its magnetic phase diagram for the geometry $\mathbf{H}\|\mathbf{c}$. One of the most intriguing features is the magnetic hysteresis anomaly, whose signature is a second peak on the magnetic hysteresis loop, that has also been observed in other many type-II high-temperature superconducting (HTSC) cuprates (see Ref. 1, and references therein), as well as in Ge/Pb superlattices[2] and organic superconductors.[3] The corresponding enhancement of the persistent current density in a field parallel to the *c* axis has been interpreted with models based on increased pinning by oxygen deficient sites,[4] effect of surface barriers,[5] vortex and defect matching,[6] and dimensional crossover.[7] In a highly anisotropic material such as Bi-2212, the mixed state can be described in terms of two-dimensional (2D) vortices (pancake vortices) which are confined to the CuO_2 planes and are coupled from one layer to another by Josephson[8] and electromagnetic[9] coupling. When the coupling is strong enough, the concept of vortex line can then be meaningful. In Bi-2212, both muon-spin rotation (μSR) and small-angle neutron scattering (SANS) experiments reveal a transition from a lattice of flux lines to a lattice of pancake vortices in a region of the (*H*,*T*) diagram which coincides with that where the magnetization second peak appears (see Ref. 10, and references therein). However, although such a dimensional crossover explanation for the fishtail feature is backed up by further experimental studies,[10] less is known about the underlying parameters which govern this transition. It is expected that for highly anisotropic compounds electromagnetic (em) coupling is the dominant coupling mechanism between pancake vortices.[9] In this case, a crossover behavior is expected for B_{cr} values around $B_{cr}=B_{em}=\Phi_0/\lambda_{ab}^2(0)$, where λ_{ab} is the London magnetic penetration depth and Φ_0 is the flux quantum. As the anisotropy γ decreases, the tunneling Josephson current effect increases and it becomes predominant when $\gamma s < \lambda_{ab}(0)$; a transition is therefore expected to occur at $B_{cr}=B_J=\Phi_0/(\gamma s)^2$, where *s* describes a length scale in the *c* direction and is associated with the repeat distance between superconducting planes or group of planes (in Bi-2212, $s=c/2\sim 15$ Å).[11]

As far as it is known, the vortex state in Bi-2212 is in the limit where electromagnetic coupling is dominant over the Josephson coupling.[9] Corroboration of this statement is given by both a recent magnetic relaxation measurement in Bi-2212 (Ref. 12) which predicted a transition at $B_{cr}=\Phi_0/\lambda_{ab}^2(0)$, and a μSR study[11] which also found such a linear relation between B_{cr} and $1/\lambda_{ab}^2(0)$.

Nevertheless, this picture has to be compared to the ''boomerang'' path foreshadowed by Uemura *et al.*,[13] and then completed through additional μSR experiments.[14,15] In this case, starting from the most underdoped state, the zero temperature μSR relaxation rate $\sigma(0) \propto n_s/m_{ab}^* \propto 1/\lambda_{ab}^2(0)$ (where n_s is the superconducting carrier pair density and m_{ab}^* is the in-plane effective mass) first increases as the doping state increases, then reaches a maximum value in the slightly overdoped region, and finally decreases as the doping level increases in the overdoped region. In other words, this $\sigma(0)$ turnback means that the curve $T_c[1/\lambda_{ab}^2(0)]$ exhibits a boomerang path. However, since the second peak field position regularly increases from the slightly underdoped to the strongly overdoped state (as shown, for instance by Kishio *et al.*[16] for Bi-2212 crystals), one must clarify this discrepancy between the proposed linear $B_{cr} \propto 1/\lambda_{ab}^2(0)$ relation, the observed proportionality of this characteristic field with the doping state and the existence of a boomerang path for the $T_c[1/\lambda_{ab}^2(0)]$ curve.

 ©1998 The American Physical Society

The growth of $Bi_2Sr_2Ca_{1-x}Y_xCu_2O_{8+\delta}$ (Bi[Y]-2212) crystals has allowed us to vary the doping state from underdoped to overdoped through the controlled substitution of Y^{3+} for Ca^{2+}.[17,18] We have thus investigated the behavior of $\lambda_{ab}(0)$, as obtained from magnetization measurements, with respect to the doping state for our series of Y-substituted Bi[Y]-2212 crystals. In this paper, we report on the evidence of a boomerang effect for the $T_c[1/\lambda_{ab}^2(0)]$ relation for Bi[Y]-2212 crystals whose doping state is controlled by both the Ca^{2+}/Y^{3+} substitution and also by oxygen pressure annealings. Our results suggest that for the most overdoped crystals, the second peak magnetic fields can no longer be explained with the electromagnetic model. However, comparison with more isotropic superconductors, such as $Tl_{0.5}Pb_{0.5}Sr_2CaCu_2O_{7+\delta}$ (Tl[Pb]-1212),[19] $Hg_{0.8}Cu_{0.2}Ba_2CuO_{4+\delta}$ (Hg[Cu]-1201),[20] and $Hg_{0.8}V_{0.2}Ba_2CuO_{4+\delta}$ (Hg[V]-1201),[21] show that even the most overdoped Bi[Y]-2212 crystals remain strongly anisotropic superconductors in contrast with the thallium-based and mercury-based materials.

II. EXPERIMENTAL

The $Bi_2Sr_2Ca_{1-x}Y_xCu_2O_{8+\delta}$ crystals used in this study were grown by a self-flux method which has been described elsewhere.[18] This earlier paper also described the structural investigations undertaken to check the quality of our crystals and to analyze their cationic compositions. In the following, the different compositions (x) of our Y-substituted single crystals will be referred to as the final analyzed crystal composition ($x=0.21$, 0.28, 0.36, and 0.43). In summary, composition analyses were determined from energy dispersive x-ray spectroscopy (EDS) with a Kevex analyzer mounted on a 200 kV electron microscope. For each batch, a representative as-grown crystal exhibiting a typical T_c was crushed to prepare the grid for electron microscopy. The compositions were established by averaging the values obtained from EDS on at least twelve fragments. For each crystal, a slight scatter in the data for the Y/Ca ratio was observed. In particular, one must emphazise that this effect is maximum for the highest yttrium concentration ($x=0.43$), and is estimated to 10%. This observation for $x=0.43$ is consistent with its broad superconducting transition ($\Delta T_c^{10-90\,\%}\sim 15$ K) in comparison with the transition of all other crystals ($0\leqslant x\leqslant 0.36$) that exhibit $\Delta T_c^{10-90\,\%}$ values in the range 3–5 K.[18] Consequently, the result obtained for the $x=0.43$ crystals precludes further extensive study on these composition. The resistivity along the c axis, denoted ρ_c, is determined by using a dc technique. Crystals were contacted by using a direct configuration. The contacts were made by attaching gold wires with a silver paint on evaporated silver stripes (two on each ab face of the crystal). The current is then applied along the c axis between two facing contacts and the voltage drop is measured parallel to it. This simple contacts configuration results in good estimate of ρ_c, as discussed in Ref. 22 for Bi-2212 crystals. The magnetic properties were investigated using a dc superconducting quantum interference device (SQUID) magnetometer with magnetic fields up to 5.5 T along the c axis. For the experimental details of the reversible and irreversible measurements, see Ref. 18. The $\lambda_{ab}(T)$ values of our crystals are deduced in the framework of the London model[23] from measurements of the isothermal magnetization versus field $M_T(H)$. A fit of these $\lambda_{ab}(T)$ data in the BCS clean limit approximation[24] leads to the extrapolated $\lambda_{ab}(0)$ values.

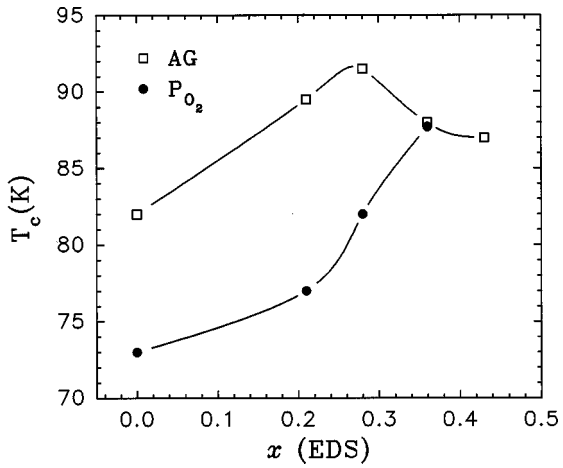

FIG. 1. T_c versus Y content x (deduced from EDS analysis) for crystals of the $Bi_2Sr_2Ca_{1-x}Y_xCu_2O_{8+\delta}$ series, as-grown (AG), and after annealing under oxygen pressure (P_{O_2}).

Concerning the irreversible measurements, the hysteresis loops of our crystals exhibit, at certain characteristic temperatures, the anomaly referred to as the fishtail effect. In the field-ascending branch, the peak of complete penetration at H_p is followed by an unexpected second peak at $H_{\max}$. A mirror image of this second peak is also observed on the reverse leg of the loop at $H'_{\max}\sim H_{\max}$. In previous studies, the $H'_{\max}$ value was found to characterize the fishtail effect (see Ref. 1, and references therein) and referred as H_{SP} (SP: second peak). This latter was usually considered to be less temperature dependent in Bi-2212 with regard to the strong dependence of its value in less anisotropic compound such as YBaCuO.[4] Nevertheless it slightly increases as T decreases. On the opposite, the $\tilde{H}$ value corresponding to the dM/dH peak is found to saturate towards low temperature as reported previously.[25] Moreover the authors of Ref. 25 observed that this low temperature value of $\tilde{H}$ coincides with the μSR crossover field $B^*(5\,\mathrm{K})$. In the following we will thus refer to $\tilde{H}$ as the characteristic field of fishtail effect.

III. RESULTS

A. Doping state in the $Bi_2Sr_2Ca_{1-x}Y_xCu_2O_{8+\delta}$ crystals

We have recently demonstrated[17,18] that substitutions of low concentrations of Y^{3+} on the Ca^{2+} site lead to a set of samples with different T_c values. The final EDS determined Y contents x and their corresponding T_c values[18] are shown in Fig. 1. We have added the data of Y-rich crystals ($x=0.43$) and those corresponding to crystals with $x=0$, 0.21, 0.28, and 0.36 which have been strongly overdoped by annealing under oxygen pressure ($P_{O_2}=100$ bar, $T=540$ °C, time$=12$ h). We interpret this development of T_c around an optimum value of 91.5 K for the as-grown crystals (see Fig. 1) in terms of a competition between two distinct phenomena. As shown previously for ceramics,[26] the increase of x is accompanied by a continuous increase of the

TABLE I. Characteristic parameters of $Bi_2Sr_2Ca_{1-x}Y_xCu_2O_{8+\delta}$ single crystals.

x	Doping state	T_c (K)	q_2	ρ_c (Ω cm)	$\lambda_{ab}(0)$ (Å)	$1/\lambda^2_{ab}(0)$ (10^7 Å^{-2})	$\Phi_0/\lambda^2_{ab}(0)$ (G)	H (G)
0.43	UD	86	4.53					210±20
0.36	UD	88	4.56	0.4±0.1	2980±10	1.13	235	250±50
0.28	~OPT	91.5	4.67	3.2±0.5	2590±15	1.49	310	
0.21	OD	89.5	4.75	4±2	1900±15	2.77	575	380±20
0	OD	82	4.84	6±2	2220±20	2.03	420	240±10
$0.28P_{O_2}$	OD	81			2280±15	1.89	400	
$0.21P_{O_2}$	OD	77			2300±15	1.92	390	550±25
$0P_{O_2}$	OD	73	4.64	0.9±0.1	2590±20	1.38	310	500±50

oxygen content. This oxygen uptake is too small to exactly compensate the Y^{3+}/Ca^{2+} valence substitution, resulting in a regular decrease in the number of holes in the CuO_2 planes as the Y content x increases. This mechanism of partial compensation tends to become less and less efficient as x increases. The initially, slightly overdoped Y-free Bi-2212 ($T_c=82$ K) can thus be driven to an optimum doping state, corresponding to $x=0.28$ ($T_c=91.5$ K), and also to the underdoped regime for higher Y contents ($x=0.43$, $T_c=86$ K). This hypothesis of increasing oxygen content with increasing x in our crystals has been confirmed from both the study of the incommensurate modulation as reflected in the value of the q_2 vector, and from transport measurements. The decrease of q_2 with increasing x ($x=0.21$, $q_2=4.75$ to $x=0.43$, $q_2=4.53$)[18] is comparable to the order of magnitude decrease observed in the $x=0$ crystal with annealing (from $q_2=4.84$ without annealing to $q_2=4.64$ after annealing under oxygen pressure) (see Table I). The similar decrease of q_2 for both Y-substituted and Y-free Bi-2212 crystals supports the hypothesis of an increased oxygen uptake with increased Y concentrations and is consistent with results reported for ceramics.[27] Moreover, previous studies in Y-free Bi-2212 crystals, report a systematic decrease of the out-of-plane resistivity $\rho_c(T=300\text{ K})$ with increasing oxygen content.[28,29] This has been ascribed to the improved metallicity of the $[BiO]_\infty$ layers (ρ_c decrease) as the oxygen content increases.[30] We indeed observed a ρ_c decrease from $\rho_c=6\pm2\ \Omega$ cm to $\rho_c\sim0.9\ \Omega$ cm after heavily doping a $x=0$ crystal, in agreement with results of Refs. 28 and 29. In this respect, although the doping level decreases as x increases, the monotonous ρ_c decrease observed in the Bi[Y]-2212 crystals, ($x=0$, $\rho_c=6\pm2\ \Omega$ cm; $x=0.36$, $\rho_c=0.4\pm0.1\ \Omega$ cm) (see Table I) confirms that the oxygen content increases with x. As a result, the as-grown, heavily Y-substituted crystals ($x=0.36$ and $x=0.43$) must already be strongly oxygenated, explaining why it is not possible to modify their T_c by annealing under oxygen pressure (see Fig. 1).

So, the Y for Ca substitution, as well as oxygen doping, provide a good way to span the whole range of doping, from the heavily overdoped to the underdoped regime. Since the HTSC's are characterized by an approximately parabolic de-

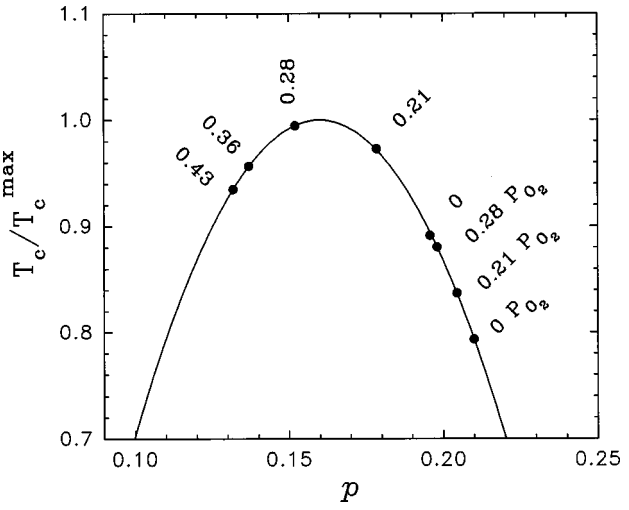

FIG. 2. T_c/T_c^{max} versus hole doping p for different as-grown Bi[Y]-2212 crystals with $x=0$, 0.21, 0.28, 0.36, and 0.43, and for P_{O_2} annealed ones denoted $0P_{O_2}$, $0.21P_{O_2}$, and $0.28P_{O_2}$. Here the curve corresponds to Eq. (1) assuming $T_c^{max}=92$ K. The p values of the different compositions x of the Bi[Y]-2212 crystals are thus deduced from the knowledge of their T_c and doping state (UD:$p<0.16$, OD:$p>0.16$).

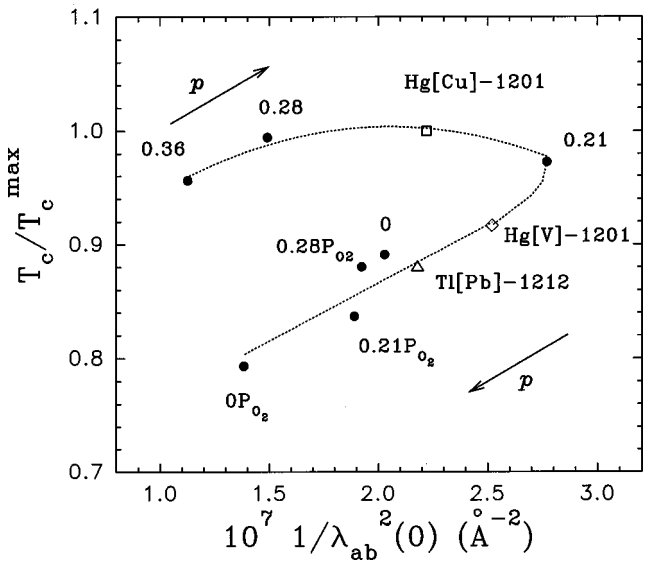

FIG. 3. $1/\lambda^2_{ab}(0)$ dependence of T_c/T_c^{max} for the Bi[Y]-2212 system (●), an optimized Hg[Cu]-1201 (□), overdoped Hg[V]-1201 (◇), and a strongly overdoped Tl[Pb]-1212 (△). The arrows point to the direction of increasing doping level p. The dashed line is a guide for the eyes.

pendence of T_c on the doping level, i.e., the hole concentration p, the above results on our Bi[Y]-2212 crystals can be summarized on a $T_c(p)$ curve. Presland *et al.*[31] showed that the relationship of $T_c/T_c^{\max}$ to p is described by the parabola

$$T_c/T_c^{\max}=1-82.6(p-0.16)^2, \quad (1)$$

which was first demonstrated for $La_{2-x}Sr_xCuO_{4+\delta}$ data, but also describes other systems as well such as $Bi_{1.9}Pb_{0.2}Sr_2Ca_{0.9}Cu_2O_{8+\delta}$.[32] Although Kato *et al.*[33] founded that in the Bi-2212 system the value of $p_{\max}\sim 0.05$, at which T_c is maximum, is smaller than the 0.16 value of Eq. (1), the shape of the $T_c(p)$ curve was found to be similar to that described by Eq. (1). Since we do not have direct information on the p values of our crystals, we have supposed that the relationship between T_c and the doping state in the Bi-2212 system, controlled through Y^{3+} for Ca^{2+} substitution and PO_2 annealing, is also conveniently approximated by Eq. (1). Then, knowing that for $x<0.28$ our crystals are overdoped (see Fig. 1 and discussion above) and assuming $T_c^{\max}$ to be 92 K, the corresponding p values are deduced from Eq. (1) for each kind of crystal. This allows us to draw qualitatively the $T_c(p)$ curve for our crystals (see Fig. 2). Nevertheless, there remains an uncertainty concerning the nearly optimized $x=0.28$ composition. The hypothesis that it is slightly underdoped (Fig. 2) will be confirmed in the following.

B. $T_c[1/\lambda_{ab}^2(0)]$: ''Boomerang''

The resulting $\lambda_{ab}(0)$ data for the $x=0$, 0.21, and 0.28 crystals annealed under oxygen pressure and for the $x=0$, 0.21, 0.28, and 0.36 as-grown crystals of Ref. 18 are reported in Fig. 3 in the form $T_c[1/\lambda_{ab}^2(0)]$ so that a direct comparison is possible with the μSR data, i.e., $T_c[\sigma(0)]$ with $\sigma(0)\propto 1/\lambda_{ab}^2(0)$. Nevertheless, since the absolute $\lambda_{ab}(0)$ values are known to strongly depend on the way they have been determined, the comparison with μSR data will remain qualitative. However, in order to validate the general trend of the observed $T_c[1/\lambda_{ab}^2(0)]$ behavior, we also added on the plot of Fig. 3 data obtained from the same type of measurements, on different crystals with well-known doping states: optimized $Hg_{0.8}Cu_{0.2}Ba_2CuO_{4+\delta}$ (Hg[Cu]-1201, $T_c=96$ K),[20] slightly overdoped $Hg_{0.8}V_{0.2}Ba_2CuO_{4+\delta}$ (Hg[V]-1201, $T_c=88$ K),[21] and overdoped $Tl_{0.5}Pb_{0.5}Sr_2CaCu_2O_{7+\delta}$ (Tl[Pb]-1212, $T_c=80$ K).[19] This T_c versus $1/\lambda_{ab}^2(0)$ curve clearly mimics the ''boomerang path'' observed by μSR measurements. In the underdoped regime, $1/\lambda_{ab}^2(0)$ increases with T_c, and thus with the number of charge carriers p, which is consistent with the $1/\lambda_{ab}^2(0)\propto n_s/m^*$ relation. In the optimally doped, as well as in the slightly overdoped region, $1/\lambda_{ab}^2(0)$ still increases with the carrier concentration; $1/\lambda_{ab}^2(0)$ reaches a maximum corresponding to $\lambda_{ab}(0)=1900\pm 15$ Å, and then starts to decline with T_c whereas p continues to increase. Thus, in the overdoped region, although the normal state carrier concentration p increases, n_s/m^* decreases. This was previously ascribed to the progressive reduction of pair lifetime arising from pair breaking.[14,34]

Although an increase of $1/\lambda_{ab}^2(0)$ with increasing p is observed in the underdoped region for our crystals (see Fig. 3) as expected from previous studies,[13–15] the lack of data in this region precludes us from drawing any comparison concerning the evolution of $1/\lambda_{ab}^2(0)$ with T_c to the ''Uemura plot''.[13] Nevertheless, in the overdoped region, $1/\lambda_{ab}^2(0)$ decreases quasilinearly with T_c as has been previously reported on overdoped ceramics of Tl-2201 (Ref. 14) from μSR measurements. The general shape of our boomerang curve suggests moreover that the nearly optimized $x=0.28$ crystal is slightly underdoped, justifying its position in Fig. 2. Finally, the rather good fit of the data for Hg and Tl-based crystals with the Bi[Y]-2212 curve, agrees well with the expected universal behavior for HTCS's.[13–15,34]

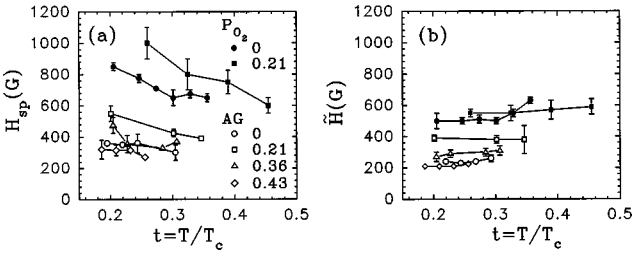

FIG. 4. Reduced temperature $t=T/T_c$ dependence of two characteristics fields of the fishtail feature in our Bi[Y]-2212 crystals with different Y content x, as-grown (AG $x=0$, 0.21, 0.36, and 0.43), and after P_{O_2} annealing (P_{O_2} $x=0$ and 0.21), (a): H_{sp} and (b): $\tilde{H}$ (see text).

C. Fishtail effect in Bi[Y]-2212, importance of the $T_c[1/\lambda_{ab}^2(0)]$ boomerang

Although it is not well understood, a common trend tends to emerge for the relationship between the fishtail position and the doping level in the superconducting cuprates. For instance, it was shown that the carriers content increase by oxygen doping or by nonisovalent cationic substitution, shifts this line to higher fields for materials in the overdoped (OD) regime of $Bi_2Sr_2CaCu_2O_{8+\delta}$,[6,16,35–37] $Tl_2Ba_2CuO_{6+\delta}$

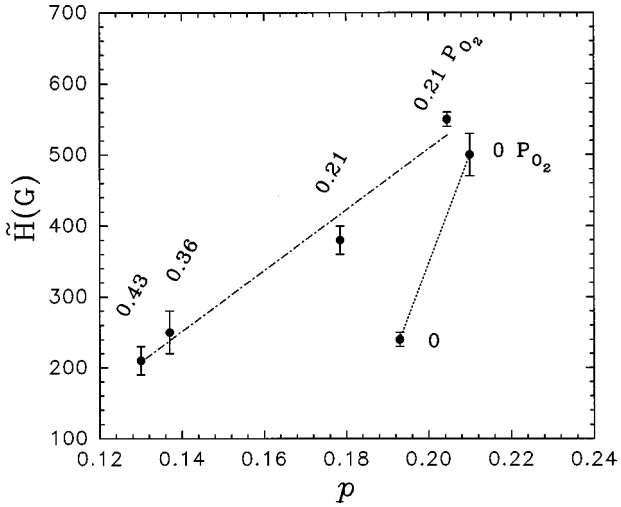

FIG. 5. Doping dependence of the characteristic field $\tilde{H}$ for the fishtail effect in the Y-substituted series $Bi_2Sr_2Ca_{1-x}Y_xCu_2O_{8+\delta}$ as well as Y-free crystal ($x=0$). Data corresponding to P_{O_2} annealed crystals ($x=0$ and $x=0.21$ P_{O_2}) are also added. The dotted lines are just guide for the eyes.

(Tl-2201),[38] and $(La_{1-x}Sr_x)_2CuO_4$ (La-214).[39] But the effect of increasing hole concentrations through anionic or cationic doping must be studied over the whole range of doping in a single system to draw out any general conclusion. A similar enhancement of the fishtail line as a response to an oxygen content increase is observed in the optimum region from the underdoped (UD) to the overdoped regime of $YBa_2Cu_3O_{7-\delta}$.[40] Another investigation of Sr doping in La-214 ranging from the UD to the OD regime supports the expected increase of the second peak field going from UD to OD regime although it did not reveal any regular behavior.[41] In the Bi-2212 system, the experimental difficulty in attaining materials in the UD regime limits this kind of study. Moreover, when this impediment has been overcome, although a transition line is still observed in μSR, no fishtail effect was observed in the UD region of Bi-2212,[25,42] except near the optimum doping.[16] This emphasizes another interesting aspect of the Y substitution which is that hysteresis loops for our crystals exhibit a well-marked second peak around 20–30 K from UD to OD. The optimum composition ($x=0.28$) being the only exception [see Figs. 4(a) and 4(b)], the lack of a fishtail in this case has been previously related to high J_c values.[17] Figure 4(a) illustrates the temperature dependence of the H_{SP} (H'_{max}) field, to be compared to the low-temperature saturation of the $\tilde{H}$ (dM/dH peak) [see Fig. 4(b)], thus justifying the choice of this latter as the characteristic field for the fishtail effect as discussed in the experimental section.

It is evident from Fig. 4(b) that the value of $\tilde{H}$ is strongly composition dependent. This is emphasized in Fig. 5 where the low-temperature value of $\tilde{H}$ is plotted against the assumed p values of the crystals. One has to bear in mind here that the p values are only qualitative. Nevertheless, two main points emerge from this figure. First of all, the Y-free ($x=0$) crystal seems to stand apart from the behavior of the Y-substituted ones. Even though the fishtail values of the most overdoped crystals ($x=0\ P_{O_2}$ and $x=0.21\ P_{O_2}$) tend to join each other for almost similar doping state, the $\tilde{H}$ values of the as-grown Y-free $x=0$ and Y-substituted crystals corresponding to smaller doping levels, do not fall on the same $\tilde{H}(p)$ curve. The possibility to get two Bi-2212 crystals exhibiting different $\tilde{H}$ values though their hole carrier content p is the same emphasizes the difference between the Ca^{2+}/Y^{3+} substituted crystals and the pure Ca Bi-2212 ones. Such an effect on the second peak suggests that p is not the only important parameter but that their different $\lambda_{ab}(0)$ values (Fig. 3) may act on the pinning properties through the vortex-vortex interactions which is λ_{ab} dependent as previously reported from μSR study of $Bi_2Sr_2Ca_{1-x}Gd_xCu_2O_{8+\delta}$ ceramics.[45] Secondly, in each series (Y-free and Y-substituted crystals), $\tilde{H}$ is found to regularly increase with p. On one hand, as x decreases in the Y-substituted series from $x=0.43$ to $x=0.21$, $\tilde{H}$ is found to increase from $\tilde{H}=210\pm20$ G to $\tilde{H}=380\pm20$ G. Furthermore, by oxygen pressure annealing, the obtained value for the most overdoped crystal of the series ($x=0.21$) keeps increasing and continues the $\tilde{H}(p)$ curve. On the other hand, the same trend, that is to say an $\tilde{H}$ increase with p is observed for the most overdoped Y-free crystal ($x=0\ P_{O_2}$), a larger $\tilde{H}$ ($\tilde{H}=500\pm30$ G) value is obtained, to be compared to $\tilde{H}=240\pm10$ G for the as-grown crystal.

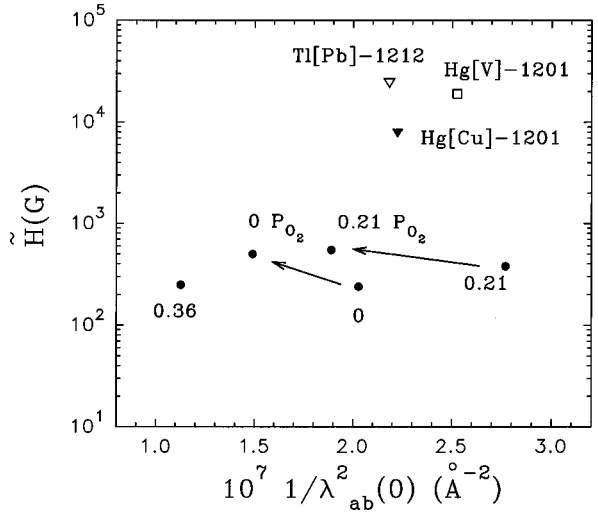

FIG. 6. Semilogarithmic representation of $\tilde{H}$ versus $1/\lambda^2_{ab}(0)$ for the Bi[Y]-2212, Hg[Cu]-1201, Hg[V]-1201, and Tl[Pb]-1212 crystals. The arrows indicate the increasing doping level obtained by oxygen pressure annealing for $x=0$ and $x=0.21$.

At this stage of the study it commands attention that the continuous increase of $\tilde{H}$ with p, from the UD regime ($x=0.43$, $x=0.36$) to the OD one ($x=0.21$, $x=0.21\ P_{O_2}$), together with the existence of a boomerang behavior of $1/\lambda^2_{ab}(0)$ with p, when going from UD to OD regime through the optimum, clearly invalidate models solely invoking a $1/\lambda^2_{ab}(0)$ dependence of $\tilde{H}$. In particular, the boomerang existence leads to two different kinds of problems. The first one is that two crystals with a same London penetration depth value $\lambda_{ab}(0)$ may be, respectively, UD and OD and thus have very different $\tilde{H}$ values. The second one is shown on Fig. 5 for $x=0$ and $x=0.21$ crystals. By oxygen pressure annealing, their overdoped character can be increased, leading to higher $\tilde{H}$ values, although $1/\lambda^2_{ab}(0)$ decreases. Consequently, it is not surprising that our $\tilde{H}[1/\lambda^2_{ab}(0)]$ data do not obey the $\tilde{H}=\Phi_0/\lambda^2_{ab}(0)$ relation which stands in the electromagnetic decoupling scenario (see Table I). Clearly, the $\tilde{H}[1/\lambda^2_{ab}(0)]$ variation for $x=0$ and $x=0.21$ (as-grown, P_{O_2}) indicated by arrows on Fig. 6 is totally opposite to that predicted by $\tilde{H}=\Phi_0/\lambda^2_{ab}(0)$. Nevertheless, in this figure one can remark that less anisotropic superconducting cuprates (Hg[Cu]-1201, Hg[V]-1201, and Tl[Pb]-1212) exhibit larger $\tilde{H}$ values than that of Bi[Y]-2212 crystals. This suggests that for the most overdoped Bi cuprate exhibiting the highest $\tilde{H}$ value of this system, $\tilde{H}$ is not only driven by $\lambda_{ab}(0)$ as suggested in the em model, but the anisotropy may be also important since it is probably decreased as the doping level is increased via oxygen pressure annealing. This result is consistent with the enhanced metallization of the insulating layers observed from resistivity measurements, which is a consequence of the introduction of oxygen in the BiO planes. Nevertheless, whatever its doping state, the values of the

Bi-2212 system lie far from those of the more isotropic systems with similar number of $[CuO_2]_\infty$ layers but with thinner interlayers such as Tl[Pb]-1212 (see Fig. 6). Thus it clearly appears that the behavior of the Bi-2212 system, although its anisotropy is affected by Y substitution or P_{O_2} annealing, remains far from those of more isotropic cuprates. This may explain why the anisotropy does not play the same role in the Bi-2212 system as for those systems as discussed in Ref. 9.

IV. CONCLUSION

The Y^{3+} for Ca^{2+} substitutions as well as P_{O_2} annealing have allowed us to explore the doping state of the Bi-2212 crystals from the underdoped regime to the overdoped one through an optimum at $T_c \sim 91.5$ K. A boomerang path $T_c[1/\lambda_{ab}^2(0)]$ has been shown for these crystals. In particular, the overdoped region of the boomerang is characterized by a $1/\lambda_{ab}^2(0)$ decrease with doping level increase as already observed on many superconducting cuprates through μSR measurements. However, for the corresponding overdoped crystals ($x=0$ and $x=0.21$) an increase of the fishtail characteristic field $\tilde{H}$ with the doping level is observed. Consequently, this $\tilde{H}$ increase as $1/\lambda_{ab}^2(0)$ decreases is totally opposite to the expected $\tilde{H}=\Phi_0/\lambda_{ab}^2(0)$ linear relation of the em model. Thus, the existence of the boomerang shape in Bi-2212 invalidates models which only involve $\lambda_{ab}^2(0)$ as the underlying parameter determining the $\tilde{H}$ position [and its corresponding transition line in the (H,T) plane]. Finally, from these experimental results it clearly appears that other parameters must be also considered in order to interpret the fishtail of Bi-2212 such as the anisotropy and disorder as proposed in Refs. 43 and 44.

[1] V. Hardy, A. Wahl, A. Ruyter, A. Maignan, C. Martin, L. Coudrier, J. Provost, and Ch. Simon, Physica C **232**, 347 (1994).

[2] D. Neerinck, K. Temst, M. Baert, E. Osquiguil, C. Van Haesendonck, Y. Bruynseraede, A. Gilabert, and I. K. Schuller, Phys. Rev. Lett. **67**, 2577 (1991).

[3] T. Tamegai, S. Ooi, M. Sato, T. Shibauchi, H. Mori, S. Tajima, and S. Tanaka, J. Low Temp. Phys. **105**, 1733 (1996).

[4] M. Daeumling, J. M. Seuntjens, and D. C. Larbalestier, Nature (London) **346**, 332 (1990).

[5] V. N. Kopylov, A. E. Koshelev, and I. F. Schegolev, Physica C **170**, 291 (1990).

[6] G. Yang, P. Shang, S. D. Sutton, I. P. Jones, J. S. Abell, and C. E. Gough, Phys. Rev. B **48**, 4054 (1993).

[7] V. M. Vinokur, P. H. Kes, and A. E. Koshelev, Physica C **168**, 29 (1990).

[8] W. E. Lawrence and S. Doniach, in *Proceedings of 12th International Conference on Low Temperature Physics*, edited by E. Kanda (Academic Press, Kyoto, 1971).

[9] G. Blatter, V. Geshkenbein, A. Larkin, and H. Nordborg, Phys. Rev. B **54**, 72 (1996).

[10] P. H. Kes, H. Pastoriza, T. W. Li, R. Cubitt, E. M. Forgan, S. L. Lee, M. Konczykowski, B. Khaykovich, D. Majer, D. T. Fuchs, and E. Zeldov, J. Phys. I **6**, 2327 (1996).

[11] C. M. Aegerter, S. L. Lee, H. Keller, E. M. Forgan, and S. H. Lloyd, Phys. Rev. B **54**, R15 661 (1996).

[12] M. Nideröst, A. Suter, P. Visani, A. C. Mota, and G. Blatter, Phys. Rev. B **53**, 9286 (1996).

[13] Y. J. Uemura, G. M. Luke, B. J. Sternlieb, J. H. Brewer, J. F. Carolan, W. N. Hardy, R. Kadono, J. R. Kempton, R. F. Kiefl, S. R. Kreitzman, P. Mulhern, T. M. Riseman, D. Ll. Williams, B. X. Yang, S. Uchida, H. Takagi, J. Gopalakrishnan, A. W. Sleight, M. A. Subramanian, C. L. Chien, M. Z. Cieplak, Gang Xiao, V. Y. Lee, B. W. Statt, C. E. Stronach, W. J. Kossler, and X. H. Yu, Phys. Rev. Lett. **62**, 2317 (1989).

[14] Ch. Niedermayer, C. Bernhard, U. Binninger, H. Glückler, J. L. Tullon, E. J. Ansaldo, and J. I. Budnick, Phys. Rev. Lett. **71**, 1764 (1993).

[15] C. Bernhard, Ch. Niedermayer, U. Binninger, A. Hofer, J. L. Tallon, G. V. M. Williams, E. J. Ansaldo, and J. I. Budnick, Physica C **226**, 250 (1994).

[16] K. Kishio, J. Shimoyama, Y. Kotaka, and K. Yamafuji (unpublished).

[17] G. Villard, D. Pelloquin, A. Maignan, and A. Wahl, Appl. Phys. Lett. **69**, 1480 (1996).

[18] G. Villard, D. Pelloquin, A. Maignan, and A. Wahl, Physica C **278**, 11 (1997).

[19] A. Wahl, A. Maignan, C. Martin, V. Hardy, J. Provost, and Ch. Simon, Phys. Rev. B **51**, 9123 (1995).

[20] D. Pelloquin, V. Hardy, A. Maignan, and B. Raveau, Physica C **273**, 205 (1997).

[21] G. Villard, D. Pelloquin, and A. Maignan, Physica C **307**, 128 (1998).

[22] V. Hardy, A. Maignan, C. Martin, F. Warmont, and J. Provost, Phys. Rev. B **56**, 130 (1997).

[23] L. N. Bulaevskii, L. Ledvij, and V. G. Kogan, Phys. Rev. Lett. **68**, 3773 (1992).

[24] B. Mülschlegel, Z. Phys. **155**, 313 (1959).

[25] C. Bernhard, C. Wenger, Ch. Niedermayer, D. M. Pooke, J. L. Tallon, Y. Kotaka, J. Shimoyama, K. Kishio, D. R. Noakes, C. E. Stronach, T. Sembiring, and E. J. Ansaldo, Phys. Rev. B **52**, R7050 (1995).

[26] A. Q. Pham, N. Merrien, A. Maignan, F. Studer, C. Michel, and B. Raveau, Physica C **210**, 350 (1993).

[27] A. Q. Pham, M. Hervieu, A. Maignan, C. Michel, J. Provost, and B. Raveau, Physica C **194**, 243 (1992).

[28] X-G. Li, X. Sun, W. Wu, Q. Chen, L. Shi, Y. Zhang, Y. Kotaka, and K. Kishio, Physica C **279**, 241 (1997).

[29] T. Watanabe, T. Fujii, and A. Matsuda, Phys. Rev. Lett. **79**, 2113 (1997).

[30] J. L. Tallon, C. Bernhard, Ch. Niedermayer, J. Shimoyama, S. Hahakura, K. Yamaura, Z. Hiroi, M. Takano, and K. Kishio, J. Low Temp. Phys. **105**, 1379 (1996).

[31] M. R. Presland, J. L. Tallon, R. G. Buckley, R. S. Liu, and N. E. Flower, Physica C **176**, 95 (1991).

[32] H. Takagi, T. Ido, S. Ishibashi, M. Uota, S. Uchida, and Y. Tokura, Phys. Rev. B **40**, 2254 (1989).

[33] M. Kato, W. Ito, Y. Koike, T. Noji, and Y. Saito, Physica C **226**, 243 (1994).

[34] J. L. Tallon, C. Bernhard, U. Binninger, A. Hofer, G. V. M. Williams, E. J. Ansaldo, J. I. Budnick, and Ch. Niedermayer,

Phys. Rev. Lett. **74**, 1008 (1995).
[35] B. Khaykovich, E. Zeldov, D. Majer, T. W. Li, P. H. Kes, and M. Konczykowski, Phys. Rev. Lett. **76**, 2555 (1996).
[36] S. Ooi, T. Tamegai, and T. Shibauchi, Physica C **259**, 280 (1996).
[37] T. Hanaguri, T. Tsuboi, A. Maeda, T. Nishizaki, N. Kobayashi, Y. Kotaka, J-I. Shimoyama, and K. Kishio, Physica C **256**, 111 (1996).
[38] F. Zuo and V. N. Kopylov, Physica C **261**, 289 (1996).
[39] M. Okuya, T. Sasagawa, T. Kimura, J. I. Shimoyama, K. Kitazawa, and K. Kishio, Physica C **271**, 265 (1996).
[40] K. Deligiannis, P. A. J. de Groot, M. Oussena, S. Pinfold, R. Langan, R. Gagnon, and L. Taillefer, Phys. Rev. Lett. **79**, 2121 (1997).
[41] Y. Kodama, K. Oka, Y. Yamaguchi, Y. Nishihara, and K. Kajimura, Phys. Rev. B **56**, 6265 (1997).
[42] X. L. Wang, J. Horvat, H. K. Liu, J. N. Li, and S. X. Dou, Phys. Rev. B **55**, R3402 (1997).
[43] B. Khaykovich, M. Konczykowski, E. Zeldov, R. A. Doyle, D. Majer, P. H. Kes, and T. W. Li, Phys. Rev. B **56**, R517 (1997).
[44] T. Giamarchi and P. Le Doussal, Phys. Rev. B **55**, 6577 (1997).
[45] P. A. J. De Groot, R. A. Rose, and B. D. Rainford, Hyperfine Interact. **86**, 591 (1994).